

CHEMISTRY

A EUROPEAN JOURNAL

Supporting Information

© Copyright Wiley-VCH Verlag GmbH & Co. KGaA, 69451 Weinheim, 2013

Synthesis, Characterization, and Reactivity of Cobalt(III)–Oxygen Complexes Bearing a Macrocyclic N-Tetramethylated Cyclam Ligand

**Doyeon Kim,^[a] Jaeheung Cho,^[a, b] Yong-Min Lee,^[a] Ritimukta Sarangi,^[c] and
Wonwoo Nam^{*[a]}**

chem_201300107_sm_miscellaneous_information.pdf

Table S1. Crystal data and structure refinements for [Co(15-TMC)(CH₃CN)₂](ClO₄)₂ and [Co(15-TMC-CH₂-O)(OH)](ClO₄)·CH₃CN.

	[Co(15-TMC)(CH ₃ CN) ₂](ClO ₄) ₂	[Co(15-TMC-CH ₂ -O)(OH)](ClO ₄)·CH ₃ CN
Empirical formula	C ₁₉ H ₀ Cl ₂ CoN ₆ O ₈	C ₁₇ H ₃₇ ClCoN ₅ O ₆
Formula weight	570.08	501.90
Temperature (K)	170(2)	170(2)
Wavelength (Å)	0.71073	0.71073
Crystal system/space group	Monoclinic, <i>P2(1)/n</i>	Monoclinic, <i>P2(1)/c</i>
Unit cell dimensions		
<i>a</i> (Å)	8.6493(8)	9.6291(3)
<i>b</i> (Å)	15.6174(13)	19.6761(6)
<i>c</i> (Å)	10.7612(9)	12.0095(4)
<i>α</i> (°)	90.00	90.00
<i>β</i> (°)	111.2190(10)	98.974(2)
<i>γ</i> (°)	90.00	90.00
Volume (Å ³)	1355.1(2)	2247.51(12)
<i>Z</i>	2	4
Calculated density (g/cm ⁻³)	1.397	1.483
Absorption coefficient (mm ⁻¹)	0.880	0.925
Reflections collected	7479	29048
Independent reflections [<i>R</i> (int)]	2636 [0.1214]	4263 [0.0349]
Refinement method	Full-matrix least-squares on <i>F</i> ²	Full-matrix least-squares on <i>F</i> ²
Data/restraints/parameters	2636/0/179	4263/0/276
Goodness-of-fit on <i>F</i> ²	1.080	1.104
Final <i>R</i> indices [<i>I</i> > 2σ(<i>I</i>)]	<i>R</i> ₁ = 0.0865, <i>wR</i> ₂ = 0.2603	<i>R</i> ₁ = 0.0699, <i>wR</i> ₂ = 0.2470
<i>R</i> indices (all data)	<i>R</i> ₁ = 0.0941, <i>wR</i> ₂ = 0.2671	<i>R</i> ₁ = 0.0875, <i>wR</i> ₂ = 0.2671
Largest difference peak and hole (e/Å ³)	1.282 and -1.048	0.941 and -0.612

Table S2. Selected bond distances (Å) and angles (°) for [Co(15-TMC)(CH₃CN)₂](ClO₄)₂ and [Co(15-TMC-CH₂-O)(OH)](ClO₄)·CH₃CN.

Bond Distances (Å)			
[Co(15-TMC)(CH ₃ CN) ₂](ClO ₄) ₂		[Co(15-TMC-O)(OH)](ClO ₄)·CH ₃ CN	
Co1-N1	2.216(4)	Co1-N1	1.988(5)
Co1-N2	2.225(4)	Co1-N2	2.125(5)
Co1-N3	2.165(5)	Co1-N3	2.089(4)
		Co1-N4	2.082(5)
		Co1-O1	1.896(3)
		Co1-O2	1.878(4)
Bond Angles (°)			
[Co(15-TMC)(CH ₃ CN) ₂](ClO ₄) ₂		[Co(15-TMC-O)(OH)](ClO ₄)·CH ₃ CN	
N1-Co1-N2	89.40(19)	N1-Co1-N2	91.1(2)
N1-Co1-N3	91.56(18)	N1-Co1-N3	171.10(18)
N2-Co1-N3	88.44(18)	N1-Co1-N4	85.0(2)
		N2-Co1-N3	92.0(2)
		N2-Co1-N4	175.5(2)
		N3-Co1-N4	92.2(2)
		N1-Co1-O1	74.04(18)
		N2-Co1-O1	91.24(16)
		N3-Co1-O1	97.56(16)
		N4-Co1-O1	89.87(15)
		N1-Co1-O2	100.09(19)
		N2-Co1-O2	85.73(18)
		N3-Co1-O2	88.46(17)
		N4-Co1-O2	92.71(17)
		Co1-O1-C1	92.7(3)
		O1-Co1-O2	173.36(17)

Table S3. Co-K Pre-edge analysis for **1**, **2**, and **3**.

	Pre-edge (1s→3d) (eV) ^a	Co K rising-edge (eV) ^b
1	7709.3(0.04) ^c	7720.4
2	7710.2(0.02)	7721.2
3	7710.2(0.02)	7721.0

^aIntensity weighted average energy of pre-edge multiplet features. ^bEnergy position of first inflection point.

^cValues in parentheses are the statistical standard deviations calculated from the individual acceptable fits used in the analysis. Fits performed using Edg-Fit (a peak fitting routine in EXAFSPAK, reference 6)

Table S4. EXAFS least squares fitting results for **2** and **3**.

Complex	Coordination/Path	R(Å) ^a	σ ² (Å ²) ^b	E ₀ (eV)	F ^c
2	2 Co-O	1.89	154	-1.88	0.18
	4 Co-N	2.07	809		
	1 Co-N	2.40	784		
	8 Co-C ^d	2.94	1150		
	16 Co-C-N ^d	3.23	/1150		
	4 Co-C	3.49	340		
3	1 Co-O	1.86	176	-4.8	0.13
	4 Co-N	2.04	742		
	1 Co-N	2.19	164		
	8 Co-C	3.04	1851		
	16 Co-C-N	3.32	/1851		
	4 Co-C	3.47	644		
	2 Co-C-N	3.25	342		
	1 Co-C-N-C	/3.25	/342		

^aThe estimated standard deviations for the distances are in the order of ± 0.02 Å. ^bThe σ² values are multiplied by 10⁵. ^cError is given by $\Sigma[(\chi_{\text{obsd}} - \chi_{\text{calcd}})^2 k^6] / \Sigma[(\chi_{\text{obsd}})^2 k^6]$. / indicates the σ² value for the path is linked to the preceding path. The S₀² factor was set at 1.

Table S5. Kinetic data obtained in the conversion of **3** (4.0 mM) to **4** performed with different amounts of HClO₄.

Amount of HClO ₄	$k_{\text{obs}}, \text{ s}^{-1}$
40 mM	$3.9(4) \times 10^{-3}$
120 mM	$3.9(3) \times 10^{-3}$
240 mM	$4.0(3) \times 10^{-3}$

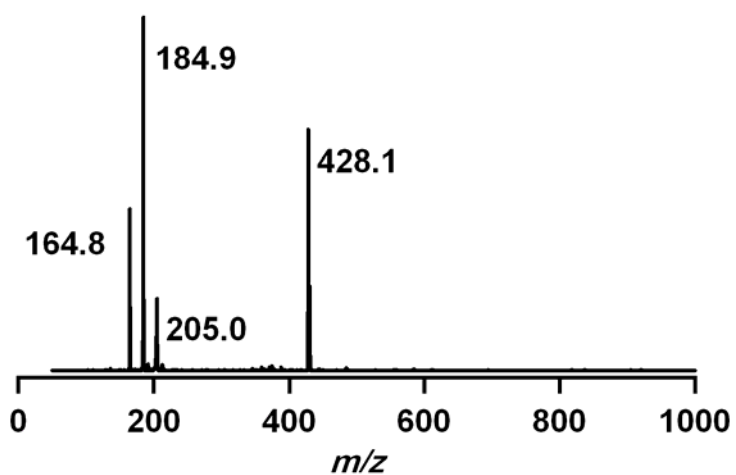


Figure S1. ESI MS of **1** in CH_3CN : Mass peaks at m/z of 164.8, 184.9, 205.0, and 428.1 are assigned to $[\text{Co}(15\text{-TMC})]^{2+}$, $[\text{Co}(15\text{-TMC})(\text{CH}_3\text{CN})]^{2+}$, $[\text{Co}(15\text{-TMC})(\text{CH}_3\text{CN})_2]^{2+}$, and $[\text{Co}(15\text{-TMC})(\text{ClO}_4)]^+$, respectively.

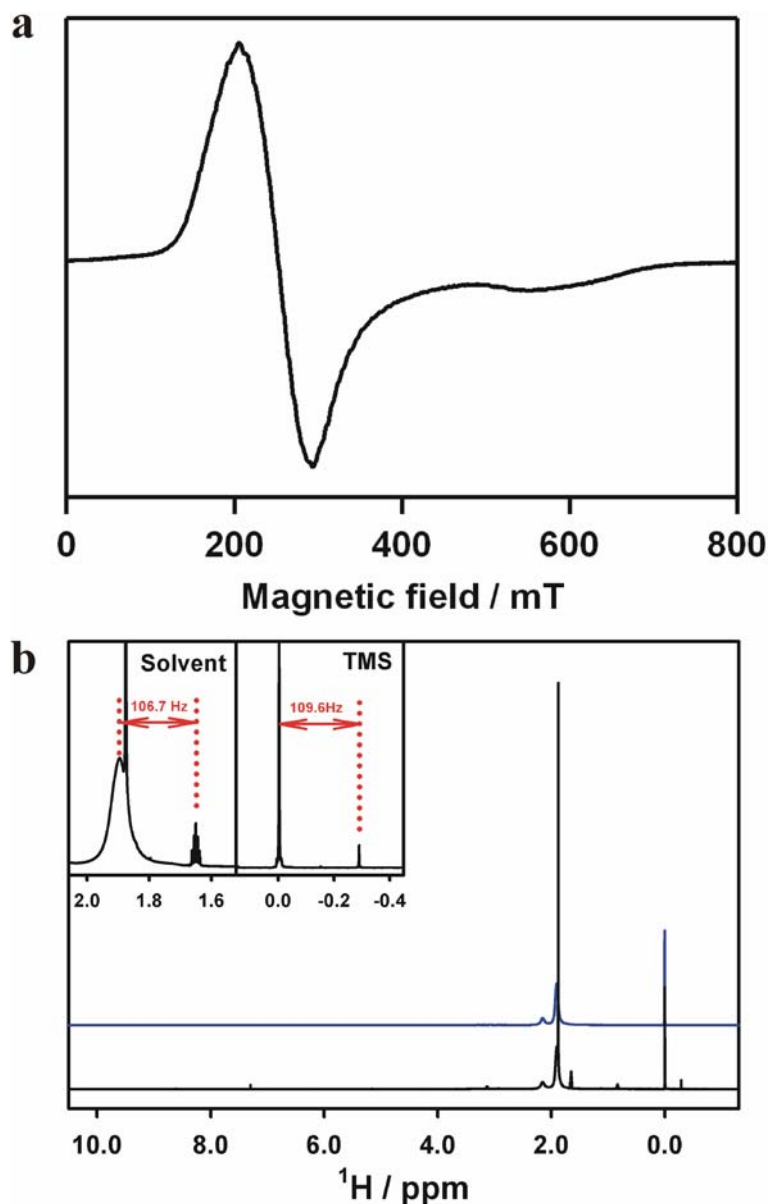


Figure S2. (a) X-band EPR spectrum of **1** (g values of 4.6 and 2.3) in frozen CH_3CN at 4.3 K. Instrumental parameters: microwave power = 1.0 mW, frequency = 9.101 GHz, sweep width = 0.5 T, modulation amplitude = 0.2 mT. (b) ^1H NMR spectra of **1** (8.0 mM) with common (blue) and Evans (black) techniques at 298 K. Insets show that the $\Delta\nu$ values of solvent and TMS peaks were 106.7 and 109.6 Hz, respectively. The magnetic moment of **1** determined to be 4.4(2) B.M. from both $\Delta\nu$ values indicates spin state of $S = 3/2$ for **1**.

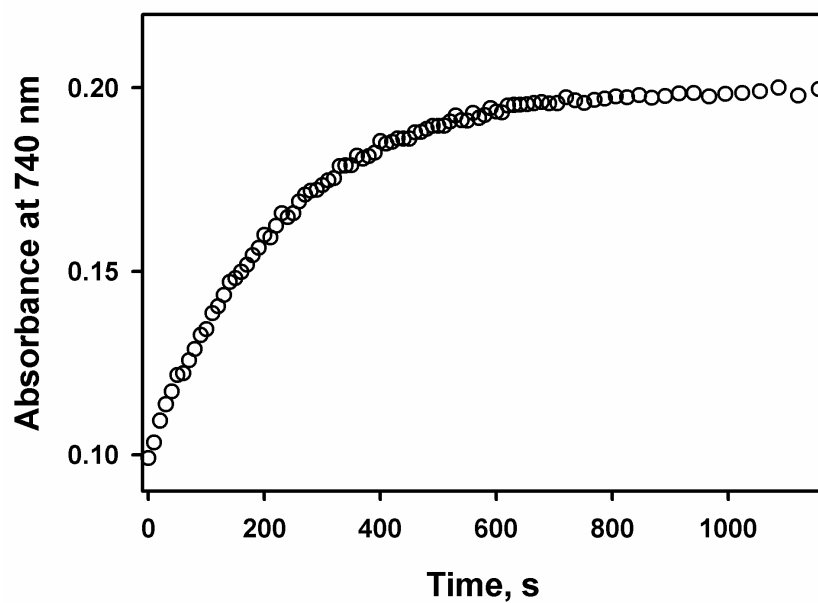


Figure S3. Time trace monitored at 740 nm in the conversion of **3** to **4** in CH₃CN at 0 °C.

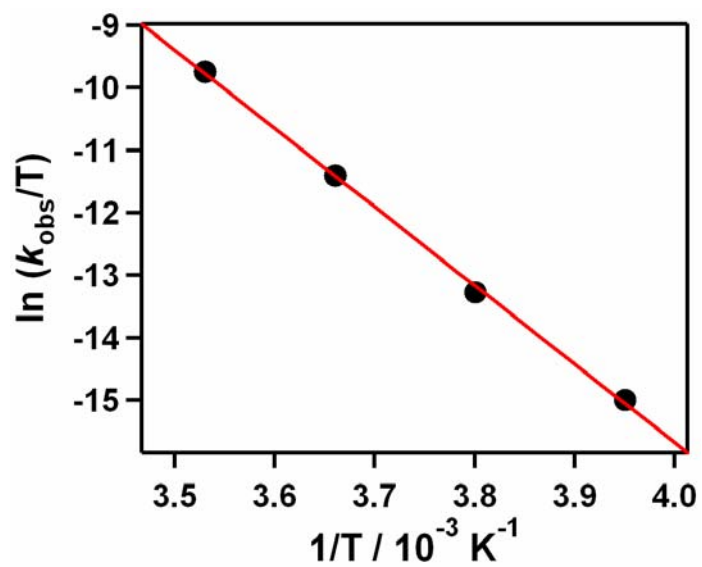


Figure S4. Plot of first-order rate constants against $1/T$ to determine activation parameters for the conversion of **3** to **4**.